Semisubsampled Wavelet Transform Based Image Watermarking with Strong Robustness to Rotation Attacks

Yingkun Hou[1,2]
[1]School of Computer Science and Technology, Nanjing University of Science and Technology, Nanjing, 210094,China
Email: sdkdhyk@163.com

Chunxia Zhao[1],Mingxia Liu[2], Zhengli Zhu[1] and Deyun Yang[2]
[2]School of Information Science and Technology, Taishan University, Taian,271021,China
Email: zhaochx@mail.njust.edu.cn

***Abstract*—In this paper, we develop a novel transform called semisubsampled wavelet transform (SSWT) and employ it to image watermarking. SSWT consists of two parts, one is nonsubsampled tight frame transform, the other is critically sampled wavelet transform (WT). Embedding watermark into the low-frequency sub-band of SSWT, the imperceptibility and robustness of watermark can be significantly improved comparing with some existing watermarking schemes. Experimental results show that proposed blind watermarking scheme is robust against JPEG compression, Gaussian noise, Wiener filtering and median filtering attacks. For rotation attack, we propose a novel watermarking resynchronization approach, the ideal watermark can be always successfully extracted after resynchronization operation to any angle rotated watermarked image. Experimental results show that the proposed resynchronization approach is considerably effective and feasible.**

***Index Terms*—semisubsampled wavelet transform, image watermarking, rotation attacks**

I. INTRODUCTION

As the rapid development of internet, multimedia security are becoming increasingly important issues [1], [2]. The watermarking system has been viewed as a possible solution to control unauthorized duplication and redistribution of those multimedia data [2]–[5]. Robustness, imperceptibility, and security are the basic requirements for a robust watermarking system [6]. Seeking new watermark embedding strategy to achieve better performance is a very challenging problem [6]. In this paper, we develop a novel image transform which is called semisubsampled wavelet transform (SSWT) and employ it to image watermarking.

For all the existing watermarking methods, the watermark can be embedded either in the spatial domain or in the transform domain, while the latter watermark embedding strategy has been demonstrated to be more robust against most of attacks [3]. We take that latter watermarking embedding strategy in our image watermark embedding scheme, particularly a binary informative watermark is embedded into the low-frequency sub-band of SSWT, higher imperceptible watermark than those traditional methods based on transform domain can be guaranteed.

For traditional critically subsampled wavelet, there are lots of watermarking schemes available. For instance, N. Bi et al. [4] proposed a watermarking scheme based on multiband wavelets transform and empirical mode decomposition (MWT-EMD) which is high robust to common signal processing attack. Lahouari et al. [7] suggested a watermarking algorithm based on the balanced multiwavelet transform and the well-established perceptual model, which is adaptive and highly robust. Ng et al. [8] put forward a maximum-likelihood detection scheme that is based on modeling the distribution of the image DWT coefficients using a Laplacian probability distribution function.

In this paper, we use the semisubsampled wavelet domain, instead of critically subsampled wavelet domain, to embed the watermark for the reason that the nonsubsampled pyramid transform via the à trous algorithm achieves shift invariance. Because the shift invariance can efficiently remove the Gibbs phenomenon, the better imperceptibility can be guaranteed, on the other hand, the higher robustness can be obtained as embedding watermark into critically sampled WT domain, due to watermark can much sufficiently spread in the reconstructed image. Besides, if watermark is just directly embedded into DWT domain, as the embedding strength increasing, the watermarked image will appear mosaic effect. However, in our method, the watermarked image can avoid this effect to a certain extent, this thanks to the nonsubsampled frame transform. Thus, watermarking imperceptibility can be further improved.

Digital watermarking robust to geometric attacks is a difficult problem that constrains the practical value of watermarking technique. Geometric attacks examples include rotation, scaling, translation etc. [9-11]. These attacks can destroy the watermark signal synchronization, so that they prevent the normal extraction of the watermark signal.

Several approaches that counterattack the general geometric attacks have been developed in recent years. These schemes [12-14] can be roughly divided into invariant transform, template insertion.

Manuscript received March 12, 2009; revised September 29, 2009; accepted October 16, 2009.
Corresponding author: Yingkun Hou

doi:10.4304/jmm.5.4.385-392

The most obvious way to achieve resilience against general geometric attacks is to use an invariant transform. In [15-17], the watermark is embedded in an affine-invariant domain by using Fourier-Mellin transformation, generalized Radon transformation, and Zernike moment, respectively. Despite that they are robust against certain global affine transformations, those techniques involving invariant domain suffer from implementation issues. Another solution to cope with general geometric attacks is to identify the transformation by retrieving artificially embedded references. In [18-19], the template is embedded in the Discrete Fourier Transform (DFT) domain as local peaks in predefined positions. The embedded local peaks are searched during the watermark detection process in order to yield information about the affine transformations that the image has undergone. However, this kind of approach can be tampered by the malicious attack since anyone can access the peaks in the DFT and easily eliminate them. Due to wavelet transform is not rotation invariant, so there is still not a efficient method to deal with geometric attack problem in wavelet domain.

In this paper, we neither embed the watermark into invariant transform domain nor embed a template into DWT transform domain, we just propose a novel watermarking resynchronization approach to resynchronize watermark in SSWT domain that undergoes any angles rotation attacks . Employ our method, the watermark is always robust to any angles rotation attack.

The rest of this paper is organized as follows. In section 2, we propose a new image transformation called semisubsampled wavelet transform. In section 3, we propose a public watermark method based on SSWT. In section 4, a novel efficiently resisting rotation attacks watermarking resynchronization algorithm is proposed. Section 5 with a large number of experiments to verify efficiency of the proposed method and algorithm. Finally, we give the conclusion of this paper in Section 6.

Your goal is to simulate the usual appearance of papers in a Journal of the Academy Publisher. We are requesting that you follow these guidelines as closely as possible.

II. SEMISUBSAMPLED WAVELET TRANSFORM

In order to remove the Gibbs phenomenon of wavelet transform, M. J. Shensa[20] proposed the nonsubsampled wavelet transform (NSWT). Due to NSWT is shift invariant, it can efficiently remove Gibbs phenomenon, this is useful for image watermarking technique to improve the watermarking imperceptibility. A. L. Cunha et al [21] proposed a NSP transform to develop a nonsubsampled contourlet transform (NSCT) based on the idea of NSWT, however, all sub-bands of NSP have the same size, watermark can not achieve sufficient spread in the reconstructed image, this is unfavorable for watermarking robustness, so we develop a novel SSWT. In our scheme, we firstly implement NSP transform, then implement critically sampled WT on the low-frequency sub-band of NSP. The watermark is embedded into the low-frequency sub-band of SSWT, the higher robustness and better imperceptibility can be obtained simultaneously.

A. NSP Transform[21]

NSP is a shift invariant filter structure, which is sub-band decomposition method similar to Laplace pyramid decomposition, it can be realized through the two channels nonsubsampled two-dimensional filter banks. Fig.1 illustrates three levels NSP decomposition. The result of the decomposition is only $J+1$ redundancy, where J is the level of decomposition, and the three levels wavelet decomposition will have $3J+1$ redundancy. At the level j of an ideal low-pass filter with support $[-(\pi/2^j),(\pi/2^j)]^2$, The corresponding ideal high-pass filter with the support is the complementation of the low-pass filter, that is $[-(\pi/2^{j-1}),(\pi/2^{j-1})]^2 \setminus [-(\pi/2^j),(\pi/2^j)]^2$. All the levels of later sequence filters are obtained through upsampling the first level filter, so one can get a multi-scale decomposition need not other filter design.

B. Nonsubsampled Pyramid Filter Banks (NSPFB)

Fig.2. displays the nonsubsampled pyramid filter banks where $H_0(z)$ and $H_1(z)$ are low-pass and high-pass decomposition filter respectively. From the analysis in [21], Finite Impulse Response (FIR) filter is easier to implement in multiple dimensions. For a general FIR two-channel NSFB, perfect reconstruction is achieved provided the filters satisfy the Bezout identity as follows:

$$H_0(Z)\bullet G_0(Z)+H_1(Z)\bullet G_1(Z)=1 \tag{1}$$

The NSPFB can be interpreted in terms of analysis/synthesis operators of frame systems. A family of vectors $\{f_i\}_{i\in N}$ constitute a frame for a Hilbert space if there exist two constants $A>0, B>0$ such that

$$A\| f \|^2 \le \sum_{i\in N} |< f, f_i >|^2 \le B\| f \|^2 \ , \quad \forall f \in H \tag{2}$$

In the event $A=B$, the frame is said to be tight. The frame bounds are the tightest positive constants satisfying (2).

Consider the NSPFB of Fig. 2. The family $\{h_0[\bullet-n], h_1[\bullet-n]\}_{n\in Z^2}$ is a frame for $l_2(Z^2)$ if and only if there exist constants $0<A<B<\infty$ such that

$$A \le \underbrace{|h_0(e^{j\omega})|^2+|h_1(e^{j\omega})|^2}_{t(e^{j\omega})} \le B. \tag{3}$$

Thus, the frame bounds of an NSPFB can be computed by

$$A=ess.\inf_{\omega\in[-\pi,\pi]^2} t(e^{j\omega}), \quad B=ess.\sup_{\omega\in[-\pi,\pi]^2} t(e^{j\omega}) \tag{4}$$

where $ess.\inf$ and $ess.\sup$ denote the essential infimum and essential supremum respectively. From (4), we see that the frame is tight whenever is almost everywhere constant.

C. SSWT Filter Banks Structure

NSP transform can implement image multi-scaledecomposition with shift invariance, shift invariance in image analysis is a very important property. However, due to upsampling, each sub-band has the same size with the original image, this is not conducive to the image watermarking. In order to improve the transparency and robustness of the watermark, we need a transformation with gradually reduced sub-band size so that the embedded watermark signal in the smaller low-frequency sub-band can obtain sufficient spread in the host image after the inverse transformation, which is conducive to enhance watermarking imperceptibility and robustness simultaneously. By the above analysis, we develop a new filtering scheme, that is, implement NSP transform to an image at first, and then implement critically sampled WT on the low-frequency sub-band of NSP, that is so called semisubsampled wavelet transform. After NSP transform, an image has the same size for all the sub-bands, one has a flexible choice of NSP transform and wavelet transform levels respectively based on the specific application. Because the wavelet filter banks holds the following Bezout identity:

$$\tilde{G}(z)\bullet G(z) + \tilde{H}(z)\bullet H(z) = 1 \tag{5}$$

So wavelet transform can be completely reconstructed; Besides, NSP transform can completely reconstruct as well, so the proposed semisubsampled wavelet filter banks can achieve perfect reconstruction. Fig. 3 gives the details of SSWT filter banks design.

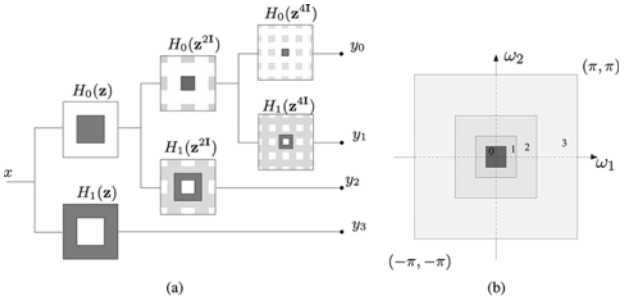

Figure 1. NSP decomposition. (a)Three-stage pyramid decomposition. The lighter gray regions denote the aliasing caused by upsampling. (b) Subbands on the 2-D frequency plane.

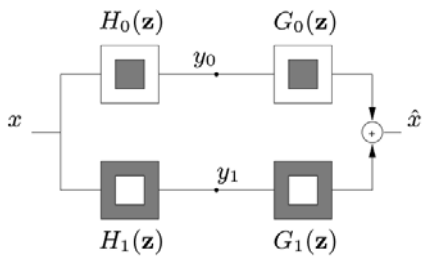

Figure 2. Nonsubsampled pyramid filter banks. The system is two times redundant and the reconstruction is error free when the filters satisfy Bezout's identity.

D. Semisubsampled Wavelet Decomposition and Reconstruction Algorithm

Given 1-D scaling filter $H_0(\xi)$ and frame filter $H_1(\xi)$, using tensor product method one constructs a 2-D scaling filter

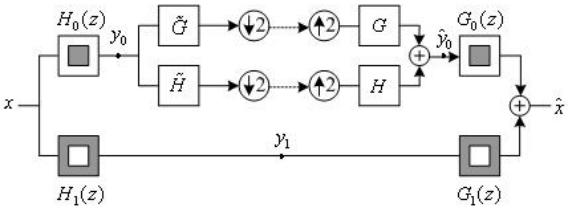

Figure 3. SSWT filter banks

$$H_{00}(\xi,\eta) = H_0(\xi)H_0(\eta) \tag{6}$$

and a 2-D frame filter

$$H_{11}(\xi,\eta) = H_1(\xi)H_1(\eta) \tag{7}$$

For the above scaling filter $H_{00}(\xi,\eta)$ and frame filter $H_{11}(\xi,\eta)$, we may use à trous [20] decomposition algorithm to decompose an image I into two subimages I_{00} and I_{11}, the subimages I_{00} and I_{11} are usually called the blurred and detailed components respectively in the NSP transform domain, then use Mallat's discrete wavelet decomposition to decompose I_{00} into four subimages. In Fig.4, we use SSWT decompose the image "Lena" with one level à trous decomposition and three levels Mallat's discrete wavelet decomposition. Where the 1-D scaling filter and frame filter for à trous decomposition are chosen as the "maxflat" filters in [21], and the 1-D scaling filter and frame filter for Mallat's discrete wavelet decomposition are chosen as "Haar" filters. In fact, the number of decomposition level for NSP and DWT in SSWT can be chosen flexibly. Besides, note that, although in the whole process of decomposition, so called nonsubsampled transform does not subsample image, but upsample the filters is always needed to obtain the multiresolution decomposition.

For image reconstruction, we use 2-D scaling filter and wavelet filter by Mallat's reconstruction method to reconstruct the subimage of NSP decomposition, then use 2-D scaling filter and dual frame filter to reconstruct original image.

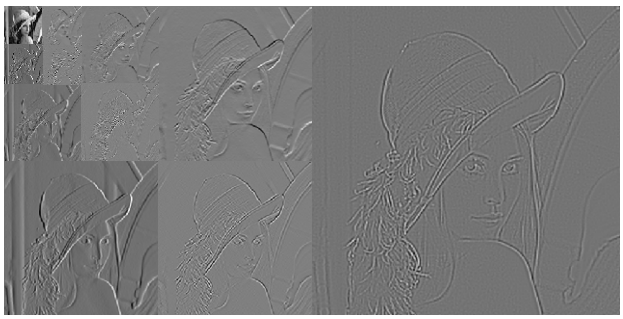

Figure 4. SSWT decomposition example, one level NSP transform and three levels DWT.

III. IMAGE WATERMARKING ALGORITHM BASED ON SSWT

In this section, we present a novel watermarking algorithm:

Step 1: Implement NSP transformation on the host image to obtain a low-frequency sub-band and a series of high-frequency sub-bands;

Step 2: Implement WT on the low-frequency sub-band to obtain a smaller low-frequency sub-band and a series of high-frequency sub-bands;

Step 3: Design a binary image watermark which has the same size with the low-frequency sub-band of step 2, embed it into low-frequency sub-band according to watermarking embedding rules.

Step 4: Implement inverse transform of the WT.

Step 5: Implement the inverse transform of NSP Transform, the watermarked image can be obtained.

A. Watermarking Embedding Algorithm

The low-frequency sub-band LL_i obtained in step 2 is a $N \times N$ coefficient matrix, design a $N \times N$ informative binary image watermark denoted as B. Embed the watermark into A, that is, implement superposition operation on A and B. The following is the information superposition algorithm:

$$A^*(i,j) = \begin{cases} A(i,j) - rem(A(i,j),S) + T_1, & if\ A(i,j) \ge 0\ and\ B(i,j) = 1; \\ A(i,j) - rem(A(i,j),S) + T_2, & if\ A(i,j) \ge 0\ and\ B(i,j) = 0; \\ A(i,j) + rem(A(i,j),S) - T_1, & if\ A(i,j) < 0\ and\ B(i,j) = 1; \\ A(i,j) + rem(A(i,j),S) - T_2, & if\ A(i,j) < 0\ and\ B(i,j) = 0. \end{cases} \tag{8}$$

Where A^* is watermarked image, T_1, T_2 are thresholds of watermark embedding, S is the embedding strength factor, take S value as big as possible under the condition of watermarking imperceptibility to improve robustness of the watermark, T_1, T_2 take $3S/4$ and $S/4$ respectively. rem is an operator similar to mod, The only difference is that mod operation rounds down (floor) but rem rounds to zero (fix):

$$rem(x,y) = x - [x/y]y \tag{9}$$

$$mod(x,y) = x - \lfloor x/y \rfloor y \tag{10}$$

B. Watermarking Extracting Algorithm

Implement Step 1 and Step 2 aforementioned on the watermarked image to obtain the low-frequency sub-band of wavelet transform and denote it as Y, by the following formula to extract the embedded watermark information:

$$Y'(i,j) = \begin{cases} 1, & if\ |rem(Y(i,j),S)| \ge (T_1 + T_2)/2; \\ 0, & if\ |rem(Y(i,j),S)| < (T_1 + T_2)/2. \end{cases} \tag{11}$$

Where Y' is the extracted watermark. S, T_1 and T_2 should take the same values as the embedding stage.

IV. Watermarking Resynchronization Algorithm to Rotation Attacks

A. Affine Transform

An image $g(x,y)$ is called the affine transform of the other image $f(x,y)$, if exist matrix $A = \begin{pmatrix} a_{11} & a_{12} \\ a_{21} & a_{22} \end{pmatrix}$ and vector $d = \begin{pmatrix} d_1 \\ d_2 \end{pmatrix}$ such that $g(x,y) = f(x_a, y_a)$, where,

$$\begin{pmatrix} x_a \\ y_a \end{pmatrix} = A \cdot \begin{pmatrix} x \\ y \end{pmatrix} + d \tag{12}$$

Obviously, rotation, scaling, translation, and shearing transforms are all the special cases of affine transformation.

For rotation attacks, $A = \begin{pmatrix} \cos\theta & \sin\theta \\ -\sin\theta & \cos\theta \end{pmatrix}$ in Eq.12, in practical implementation, due to the oblique directional interpolation must be involved, so the size of the image will have different changes after rotation transformation between the odd and even size of original image. Given an image with the size $M \times N$, let $B = \begin{pmatrix} -\frac{M-1}{2} & \frac{N-1}{2} \\ \frac{M-1}{2} & \frac{N-1}{2} \end{pmatrix}$, denote rotated image size as $M' \times N'$, then the formula for calculating M', N' is as following:

$$\begin{pmatrix} M' \\ N' \end{pmatrix} = 4\left\lceil \max(|B \bullet A|)/2 \right\rceil + \begin{pmatrix} 1 \\ 1 \end{pmatrix} \tag{13}$$

From Eq.13, we can see that whether the size of original image is odd or even, the size of rotated image will be odd. It will lead to different results for watermarking extracting after rotation attacks due to different parity of image size. We will discuss that in section 4.2.

B. Watermarking Resynchronization Algorithm to Rotation Attacks

a) Rotation Attacks Model

Given a $(2n+1) \times (2n+1), n \in N$ image I, after random angle θ rotation, we can see that the size of the resulting image is still odd by Eq.13, if rotate the resulting image by $-\theta$, then still get an odd size image, i.e. a $(2n'+1) \times (2n'+1), n' \in N$ image I_r, the size difference between I and I_r is:

$$d_{even} = 2(n' - n). \quad (14)$$

Since d_{even} is an even number, there are $n' - n$ additive pixels around the image respectively. One can crop out the informative part from the center of I_r that has not any pixel deviation, the details is shown in Fig.5(a).

If a given image I is $2n \times 2n, n \in N$, the situation will be completely different, this because with an any angle θ rotation, the size of resulting image will be odd, and then rotate the resulting image, we still get an odd size image I_r, i.e., a $(2n'+1) \times (2n'+1), n' \in N$, the size difference between I and I_r is:

$$d_{odd} = 2(n' - n) + 1. \quad (15)$$

d_{odd} is obviously an odd number, so there are not integer pixels added around the resulting image, no matter how to crop, one can only get an image that has 0.5 pixel deviation with original image, thus, watermark is desynchronized, see Fig.5(b).

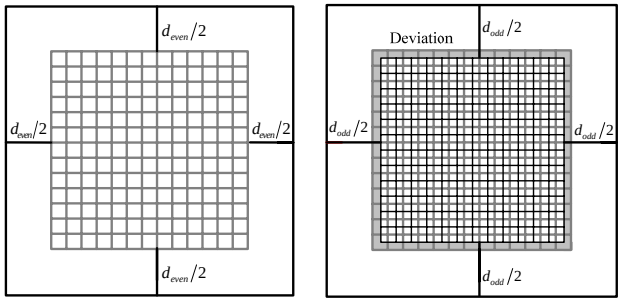

(a) (b)

Figure 5. Model of desynchronizing watermark by rotation attacks. (a) Odd size image; (b) Even size image (gray filled bands are pixel location deviation).

b) Watermarking Resynchronization Algorithm

From the model in section 4.2.1, we can see that watermark embedded into the odd size image can resynchronized only by rotating the attacked image back to original situation, then crop it out from the resulting image; for even size image, only rotate it back, there will be 0.5 pixel deviation incurred. If this deviation can not removed, the watermark could not always be extracted successfully. In this paper, we propose an efficient method to remove the deviation. Based on the aforementioned model, because the corrected image size is odd, if we crop out the informative part with the same size as original image and then implement rotation and counter rotation process once again with any angle, the deviation can be removed. This because repeat two times rotation and counter rotation, two 0.5 pixel deviation can be incurred, the sum is 1, sub-pixel deviation has already been removed. If we crop out the informative part from the resulting image, the watermark can be resynchronized. According to the above analysis, we give the watermarking resynchronization algorithm as follows:

Let A be an watermarked image with size $N \times N$, A' is the rotated version of A with an angle θ, the size of A' is $N' \times N'$.

Step 1: If θ is known, go to step 3.

Step 2: If θ is unknown, estimate it, estimated value is denoted as θ'. The estimate formula is as the following:

$$\theta' = \begin{cases} \arcsin\dfrac{N'-1}{\sqrt{2}N} - 45^\circ, & if\ 0^\circ \le \theta \le 45^\circ; \\ 135^\circ - \arcsin\dfrac{N'-1}{\sqrt{2}N}, & if\ 45^\circ < \theta \le 90^\circ. \end{cases} \quad (16)$$

The estimation error $\theta' - \theta$ is denoted as ε, in our experiments, we take ε as $\pm 1^\circ$. Because there is an error, if one want to get the accurate value, a local searching algorithm is needed, the searching range is $\left[\theta' - 1^\circ, \theta' + 1^\circ\right]$, in our simulation, the step length is set to 0.01°.

Step 3: Rotate A' with $-\theta'$ to obtain corrected image A'' with size $N'' \times N''$, calculate the starting point (r, c) to crop out the image with size $N \times N$ by the following formula:

$$(r, c) = \left(\left\lfloor \frac{N' - N}{2} \right\rfloor + 1, \left\lfloor \frac{N' - N}{2} \right\rfloor + 1 \right) \quad (17)$$

Then crop out the informative part denoted as A''' from A''. If the size of original image is odd, go to step 5.

Step 4: Rotate the image A''' with any angle ω, the size of the resulting image is $M \times M$, and then rotate the resulting image with $-\omega$ getting image B with size $M' \times M'$, crop out the informative part from B to get the final $N \times N$ image B' with the starting point (r', c') as the following:

$$(r', c') = \left(\left\lfloor \frac{M' - M}{2} \right\rfloor + 2, \left\lfloor \frac{M' - M}{2} \right\rfloor + 2 \right) \quad (18)$$

Step 5: Extract the watermark from B' by the watermarking extracting algorithm in section 3.2.

V. EXPERIMENTAL RESULTS

In all the experiments, NSP transform is 2 levels, wavelet transform is 5 levels, the Haar wavelet basis is used in wavelet transform.

A number of experiments are conducted for 512×512 Lena, Barbara, Baboon and Peppers images employing the aforementioned methods. A binary image is used as watermark, Fig.6 shows watermarked images. In order to demonstrate the effectiveness of the proposed methods, we compare our method with the traditional wavelet based watermarking algorithm. We use bit error rate (BER) and peak signal to noise ratio (PSNR) to assess watermarking robustness and imperceptibility respectively. The formula to compute PSNR is as the following:

$$PSNR = 10\log_{10}[x_{\max}^2 /(M_1 \times M_2 \times \sum_{i=1}^{M_1}\sum_{j=1}^{M_2}(x(i,j)-y(i,j))^2] \quad (19)$$

A. Imperceptibility

Using our method, when embedding strength factor S takes 55.2 for Lena image, BER value can reach 0, PSNR value is 52.4672; but for the algorithm based on critically sampled WT, if BER can achieve 0, S takes at least 64.4 , PSNR value is only 51.0415. With the increasing S value, PSNR will be smaller and smaller, that is, the quality of watermarked will decline. The PSNR obtained by our algorithm is always bigger than the algorithm based on WT when take the same S. We implement the BER experiments under different S , To compare with the method based on critically sampled WT , we use the same watermarking embedding rules as our method and embed the same watermark into low-frequency sub-band of 5 levels WT. The BER comparison under different S between our watermarking strategy and the method based on critically sampled WT see Table 1.

Figure 6. Watermarked image (All PSNRs >52).

B. Robustness to Common Signal Processing Attacks

We present results for the study of the robustness of the proposed watermarking system against typical attacks namely Additive White Gaussian Noise(AWGN), median filtering, Wiener filtering, and JPEG compression.

To compare our watermarking algorithm with the watermarking scheme based on SSWT and the well-established perceptual model in [7] and the MWT-EMD watermarking method in [4], we perform the simulation to embed same watermark with 256 bits and PSNR (38 dB) for the watermarked image (instead of 52.4672 dB in our demonstration simulation) as in [7] into the "Lena" image. For every image and every kind of attacks, we conduct 10000 times experiments then calculate the mean as our the final results.

For AWGN, the results shown in Fig.7 clearly indicate that the proposed scheme is able to withstand AWGN attacks. Using the same watermark, results for the robustness of the proposed scheme against median filtering are shown in Fig.8. The median filtering is applied using a window of size $3\times3, 5\times5$ and 7×7 , respectively. Fig.9 illustrates results for the mean performance of the decoder in the presence of Wiener filtering. Finally, we present results for the performance of the proposed watermarking system in the presence of JPEG compression. The robustness of the proposed system against JPEG compression is clearly demonstrated in Fig. 10.

C. Robustness to Rotation Attacks

Rotate watermarked image with randomly selected angle, we only use the size of the original image and rotated image to estimate the rotation angle by Eq.16, then use a local searching algorithm to implement the resynchronization to rotation attacks in section 4.2.2. The searching range is $\left[\theta'-1^\circ, \theta'+1^\circ\right]$, step length is 0.01. In the course of searching to extract watermark, get 201 watermarks, then select optimal one as the result.

The resynchronization process is shown in Fig. 11. The BERs of extracted watermarks and the BERs given by [4] are listed in table 2.

TABLE I
BER OF EXTRACTED WATERMARK UNDER DIFFERENT S AND COMPARISON WITH CRITICALLY SAMPLED WT WATERMAKING METHOD.

S	52	54	56	58	60	62	64
Lena (SSWT)	0.0039	0.0039	0	0	0	0	0
Lena (WT)	0.0977	0.1328	0.0508	0.0391	0.0352	0.0156	0
Baboon (SSWT)	0.0195	0	0	0	0	0	0
Baboon (WT)	0.1367	0.0859	0.0781	0.0547	0.0469	0.0156	0.0039
Peppers(SSWT)	0.0156	0.0117	0	0	0	0	0
Peppers(WT)	0.1055	0.1055	0.0664	0.0781	0.0313	0.0078	0
Barbara(SSWT)	0.0078	0	0	0	0	0	0
Barbara(WT)	0.1406	0.0547	0.0859	0.0586	0.0195	0.0156	0

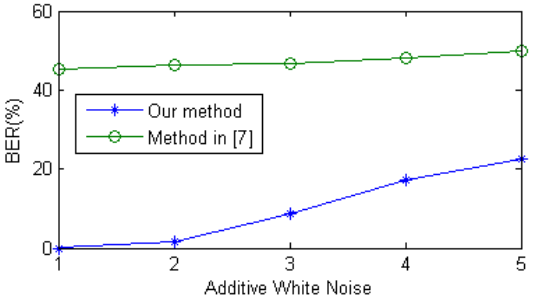

Figure 7. BERs to extract watermarks using our watermarking scheme and the method in [7] in the presence of Gaussian noise attacks with additive noise variance from 1 to 5.

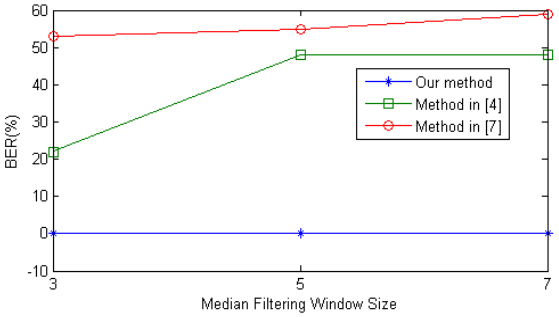

Figure 8. BERs to extract watermarks using our watermarking scheme and the methods in [4] and [7] in the presence of the median filtering attack with filter length 3, 5, and 7.

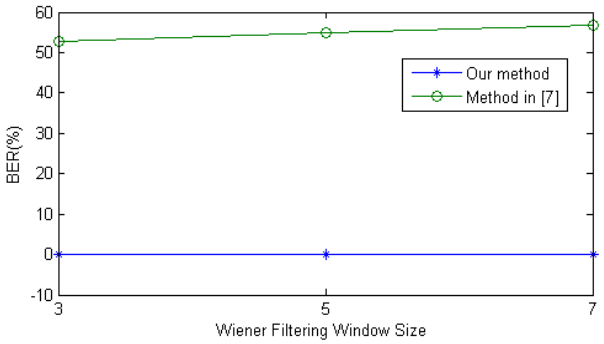

Figure 9. BERs to extract watermarks using our watermarking scheme and the method in [7] in the presence of the Wiener filtering attack with filter length 3, 5, and 7.

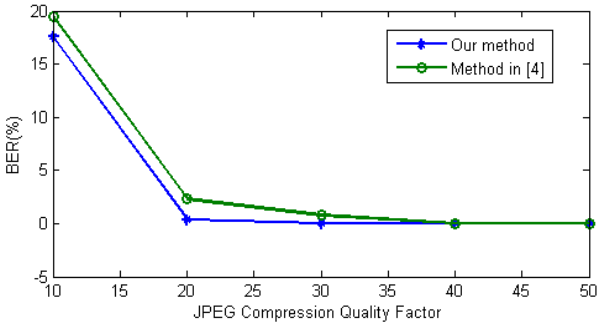

Figure 10. BERs to extract watermarks using our watermarking scheme and the method in [4] in the presence of the JPEG compression with JPEG quality factor from 10 to 50.

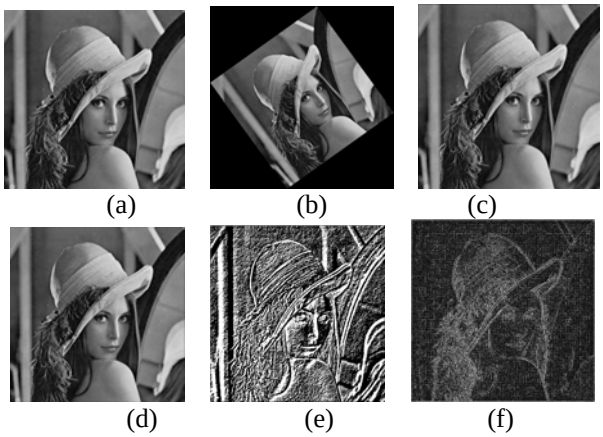

Figure 11. Watermarking resynchronization process to rotation attacks. (a) Original watermarked image; (b) Rotated image with angle 35.8°; (c) Resulting image of step 3 in section 4.2.2; (d) Resulting image of step 4 in section 4.2.2; (e) The difference between (a) and (c); (f) The difference between (a) and (d);

TABLE II
BER OF EXTRACTED WATERMARK UNDER ROTATION ATTACK AND COMPARISON WITH [4]

Angles of rotation	-2°	-1°	-0.5°	0.5°	1°	2°	5°	12.8°	34.7°	76.5°
Lena (SSWT)	0	0	0	0	0	0	0	0	0	0
Lena (in [4])	43.75	57.81	45.31	43.75	53.13	60.94	/	/	/	/
Baboon (SSWT)	0	0	0	0	0	0	0	0	0	0
Baboon (in [4])	56.25	54.69	43.75	45.31	53.13	43.75	/	/	/	/
Peppers(SSWT)	0	0	0	0	0	0	0	0	0	0
Peppers(in [4])	62.50	54.69	43.75	40.63	62.50	48.44	/	/	/	/

VI. CONCLUSIONS

In this paper, we develop a novel transform called SSWT by combining NSP tight frame transform with critically sampled WT. We employ it to image watermarking technique and proposed a novel watermarking algorithm to achieve higher robustness and better imperceptibility. The experimental results showed that our watermarking scheme is considerably effective comparing with some existing state-of-the-art watermarking algorithms in transform domain. For the robustness of watermarking to rotation attack, we give the

rotation attack desynchronize watermarking model and propose a novel watermarking resynchronization algorithm to rotation attack, experimental results show that the proposed resynchronization algorithm is considerably effective and feasible.

ACKNOWLEDGMENT

The work was supported by the National Natural Science Foundation of China(Grant No. 60572113) and Taishan University project(Y06-2-02).

REFERENCES

[1] M. Lesk, "The good, the bad, and the ugly: What might change if we had good DRM," *IEEE Security Privacy Mag.*, vol. 1, pp. 63–66, May/Jun. 2003.
[2] F. Hartung, F. Ramme, "Digital right management and watermarking of multimedia content for m-commerce applications," *IEEE Commun. Mag.*, vol. 38, pp. 78–84, Nov. 2000.
[3] I. J. Cox, J. Kilian, F. T. Leighton, T. Shamoon, "Secure spread spectrum watermarking for multimedia," *IEEE Trans. Image Process.*, vol. 6, pp. 1673–1687, Dec. 1997.
[4] N. Bi, Q.Y. Sun, D.R. Huang, Z. H. Yang, and J.W. Huang, "Robust Image Watermarking Based on Multiband Wavelets and Empirical Mode Decomposition," *IEEE Trans. Image Process.*, vol.16, pp.1956-1966, Aug. 2007.
[5] S. H. Wang and Y. P. Lin, "Wavelet tree quantization for copyright protection watermarking," *IEEE Trans. Image Process.*, vol. 13, pp. 154–165, Feb. 2004.
[6] I. J. Cox and M. L. Miller, "The first 50 years of electronic watermarking," *J. Appl. Signal Process.*, vol. 2, pp. 126–132, 2002.
[7] G. Lahouari, B. Ahmed, K. I. Mohammad, and B. Said, "Digital image watermarking using balanced multiwavelets," *IEEE Trans. Signal Process.*, vol. 54, pp. 1519–1536, Apr. 2006.
[8] T. M. Ng and H. K. Garg, "Maximum-likelihood detection in DWT domain image watermarking using Laplacian modeling," *IEEE Signal Process. Lett.*, vol. 12, pp. 345–348, Apr. 2005.
[9] F. A. P. Petitcolas, R. J. Anderson, M. G. Kuhn, "Attacks on copyright marking systems," *Proc. Workshop Information Hiding*, Portland, OR, 15–17, 1998.
[10] M. Kutter , F. A. P. Petitcolas, "A fair benchmark for image watermarking systems," *Presented at the Electronic Imaging, Security and Watermarking of Multimedia Contents*, vol. 3657, Sans Jose, CA, Jan. 1999.
[11] I. J. Cox ,J. P. M. G. Linnartz, "Public watermarks and resistance to tampering," *Presented at the IEEE Int. Conf. Image Processing*, vol. 3, 1997.
[12] V. Licks, R. Jordan, "Geometric attacks on image watermarking system," *IEEE Multimedia*, vol. 12, pp. 68-78, Jul-Sep. 2005.
[13] Liu Jiu-fen, Huang Da-ren and Huang Ji-Wu, "Survey on Watermarking against Geometric At-tack," *Journal of Electronics and Information Technology*, vol. 26, pp. 1495-1503, Sep. 2004.
[14] Dong Ping, G.B. Jovan, P.G. Nikolas, Yang Yongyi, D. Franck, "Digital watermarking robust to geometric distortions," *IEEE Trans. Image Process.*, vol. 14, pp. 2140-2150, Dec. 2005.
[15] O' Ruanaidh J J K, Pun T, "Rotation, scale and translation invariant spread spectrum digital image watermarking," *Signal processing*, vol. 66, pp. 303-317, Mar. 1998.
[16] D. Simitopoulos, D.E. Koutsonanos, "Robust image watermarking based on generalized radon transformations," *IEEE Trans. on Circuits and Systems for Video Technology*, vol. 13, pp. 732-745, Aug. 2003.
[17] H.S. Kim, H.K. Lee, "Invariant image watermarking using zernike moments," *IEEE Trans. on Circuits and Systems for Video Technology*, vol. 13, pp.766-775, Aug. 2003.
[18] S. Pereira, J.J.K. O' Ruanaidh, et al., "Secure robust digital watermarking using the lapped orthogonal transform," *IST/SPIE Electronic Image ' 99, Session: Security and Watermarking of Multimedia Contents*, San Jose, CA, USA, Jan. 1999.
[19] Xiangui Kang, Jiwu Huang, et al., "A DWT-DFT composite watermarking scheme robust to both affine transform and JPEG compression," *IEEE Trans. on Circuits and Systems for Video Technology*, vol. 13, pp. 776-786, Aug. 2003.
[20] M. J. Shensa, "The discrete wavelet transform: Wedding the à trous and Mallat algorithms," *IEEE Trans. Signal Process.*, vol. 40, pp. 2464–2482, Oct. 1992.
[21] A. L. Cunha, J.P. Zhou and Minh N. Do, "The Nonsubsampled Contourlet Transform: Theory, Design, and Applications," *IEEE Trans. Image Process.*, vol. 15, pp. 3089-3101, Otc. 2006.

Yingkun Hou received the M.S. degree in applied mathematics form Shandong University of Science and Technology, China, in 2006. He is currently pursuing the Ph.D. degree in pattern recognition and intelligent system at Nanjing University of Science and Technology.

Since 2006, he has been on the faculty in information science and technology school at Taishan University, and he is currently a lecturer in the school of information science and technology. His research interests include multimedia information security, and pattern recognition.

Chunxia Zhao was born in 1964. She received the Ph.D. degree in mechatronic control and automation at Harbin Institute of Technology in 1998.

She is a professor and doctoral supervisor at Nanjing University of Science and Technology, and the senior member of CCF. Her research interests include pattern recognition and artificial intelligence.